Benchmarking and Refining the Vaporizing Foil Actuator Spot Welding Process

A. Vivek*, S. M. Wright, B. C. Liu, S. R. Hansen, R. C. Brune, B. P. Thurston, G. A. Taber, T. Lee, Y. Mao, T. J. Dittrich, G. S. Daehn

Department of Materials Science and Engineering, The Ohio State University, USA
*Corresponding author. Email: vivek.4@osu.edu

Abstract

Impact spot welding implemented by the vaporizing foil actuator welding method has been studied. With significantly lower input energy levels as compared to resistance spot welding, similar and dissimilar lap welding of aluminium alloys (AA) of types 5052 and 7075 was implemented. The dissimilar welds between 2 mm thick AA5052 and 2.3 mm thick AA7075 were created with 4 kilojoules input energy, whereas the similar welds between 1 mm thick AA5052 sheets required only 0.6 kilojoules. Flyer sheet velocities of approximately 750 m/s were measured with a PDV system. Microhardness measurements, performed across the dissimilar weld interfaces, showed no softening of the base materials due to the welding process. A few distinct welding configurations were investigated for improving process feasibility and obtaining the highest possible weld strength. Lap shear tests and pry tests revealed that the configuration of the starting weld geometry greatly affected weld quality.

Keywords

Aluminum, Welding, Photonic Doppler velocimetry

1 Introduction

Conventional welding by means of high heat input, fusion and solidification greatly alters the microstructure in the welded region and can be detrimental to the weld's mechanical properties, especially in case of heavily engineered, high specific-strength materials (Hwang & Chou, 1998). The strength of the heat affected zone (HAZ) can be less than one

third the original strength of the base material. Additionally, susceptibility to corrosion is greatly increased after welding certain alloys such as 6xxx and 7xxx series aluminium alloys. Besides, aluminium welding requires high power, resulting in high energy consumption. Fasteners and structural adhesives offer non-welding joining solutions (Barnes & Pashby, 2000; Loureiro et al., 2010). Solid state welding techniques, such as impact welding (Y. Zhang et al., 2011), friction stir welding (Nandan et al., 2008), ultrasonic welding (C. (Sam) Zhanget al., 2009), and roll bonding (Lee et al., 2002) are a few alternatives to fusion based welding and have undergone a certain degree of industrial adaptation so far. Impact welding is of particular interest due to the potentially short cycle time of the process, the possibility to join a wide variety of metal combinations, and the ability to perform the process over varying length scales.

Vaporizing foil actuator welding (VFAW, or VFA welding) is a novel impact welding technique that utilizes the force generated by a thin aluminium foil vaporized by high electric current to launch one piece of metal toward one or more stationary target sheets (Vivek et al., 2013). Explosive welding (EXW) (Grignon et al., 2004) and magnetic pulse welding (MPW) (Watanabe & Kumai, 2009) are previously known and practiced methods of impact welding. Implementation of EXW in traditional factory environment is not possible due to safety regulation in transportation, storage and handling of explosives and because of an inability to automate such process. EXW is mostly used for welding thick plates for the shipbuilding, nuclear, oil and gas and locomotive industries. VFAW operates at the same size scale as MPW while having certain advantages over it. Longevity of the solenoid actuator used for MPW is a major concern, whereas VFAW is designed to have a low-cost consumable actuator for each cycle. With VFAW, pressures generated and achievable flyer sheet velocities are much higher as compared to MPW; therefore, a wider variety of materials can be effectively welded with VFAW. VFAW has been shown to be a significantly more efficient impact welding process as compared to MPW (Hahn et al., 2016). By changing the shape of the foil actuator and the air gap between the flyer and target sheets, welds of different shapes can be created. Circular spot welds are particularly interesting because there are existing spot welding techniques such as resistance spot welding (RSW) and friction stir spot welding (FSSW) against which VFAW can be benchmarked. In this work, spot welding of aluminium alloy type 5052 to itself and to aluminium alloy 7075 has been performed. AA5052 is a wrought aluminium alloy with ultimate tensile strength of about 228 MPa, and AA7075 is a wrought aluminium alloy with ultimate tensile strength of about 572 MPa. The similar material weld strengths have been compared to the FSSW data from Zhang et al. (2011) because they had a similar spot size of 10 mm as the work presented here. The strength data can also be compared to the data from Freeney et al. (2006), who obtained slightly higher weld strength, but their spot diameter was 12 mm.

2 Experimental Procedure

A schematic of the basic VFAW process is shown in Fig. 1. A thin aluminium foil as shown in the figure was connected across the terminals of a capacitor bank, which can be

charged up to a certain energy level. Once this energy was discharged through the foil, the foil vaporized rapidly and formed a high temperature gas that could be used to push the flyer sheet. Some degree of confinement is essential; accordingly, the other side the foil was backed by a block of steel approximately 20 mm thick. The flyer sheet has to be separated from the target sheet by an air gap, or standoff, in order to provide room for acceleration and allow for an oblique impact between the two joint members. This standoff was created by inserting an annular spacer or by pre-forming a well of certain depth into the flyer sheet (Fig. 2). The target plate was backed by another block of steel about 20 mm thick. The in-plane dimensions of the flyer as well as the target plates were 40 mm x 120 mm. The two were overlapped by 40 mm along the length and the welding experiment was conducted to create lap-welded specimens. The details of the similar and dissimilar welding are given in the subsections below. Informal pry tests, which involved uninstrumented destruction of the weld using hand tools, were conducted for preliminary screening and determination of suitable welding parameters. If the sample fractured very easily and through the interface, the parameters were changed until the pry test left a weld nugget. The lap-shear strengths of the formal samples were measured on an MTS 831.10 load frame moving with a cross-head speed of 0.1 mm/sec. For each type of sample, five were mechanically tested while one was saved for microanalysis in as-welded condition.

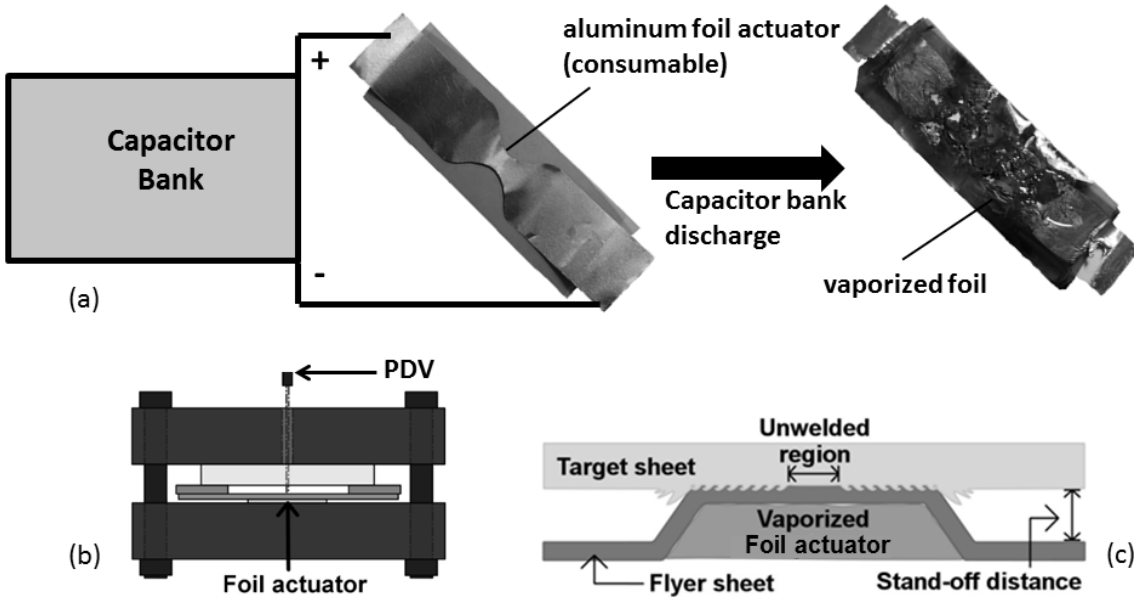

***Figure 1**: Schematics of the VFAW process: (a) the before and after experiment conditions of the foil actuator, (b) stack-up of a typical VFAW assembly, (c) close-up view of the welding operation*

In separate experiments, velocities of both AA5052-H32 and AA7075-T6 as the flyer sheets were measured using the photonic Doppler velocimeter [3]. In this experiment, the target plate had a through hole, which provided a line of sight to the laser focusing probe. With this technique, the evolution of the flyer sheet velocity can be measured with a sub-microsecond temporal resolution. Voltage was measured using a 1000V:1V probe

connected across the terminals of the capacitor bank, and current was measured by a 50kA:1V Rogowski coil.

2.1 AA5052 to AA5052

For similar welding of AA5052, 1 mm thick sheets were used as flyer as well as target sheets. Two types of samples with starting geometries as shown in Fig. 2 were created for this combination. Twelve samples were created with circular standoff (type 1) and six were created with a preformed flyer (type 2). In both cases the standoff gap was kept at 2.5 mm. Six of the type 1 samples were flattened in a hydraulic press with a force of 5 kN to remove the gap left by the standoff insert. These samples were created with an input energy of 0.6 kilojoules supplied by a custom-made capacitor bank (fast bank) that supplies a maximum energy of 1.3 kJ and has a short circuit rise time of 5 µs.

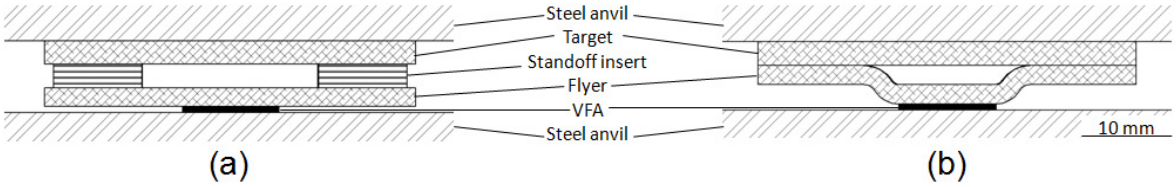

***Figure 2**: Schematic of welding stack up: (a) with standoff insert, (b) with preformed flyer sheet. Length scale is approximate.*

2.2 AA5052 to AA7075

For dissimilar welding, of AA5052 to AA7075-T6, 2 mm thick AA5052 sheets and 2.3 mm thick AA7075-T6 sheets were used. Both materials were attempted as flyer sheet. Upon pry tests of welds created, it was found that using AA5052 as the flyer sheet results in stronger welds at an energy level of 4 kJ. These experiments were conducted with a Maxwell Magneform capacitor bank (slow bank) that has a maximum charging energy of 16 kJ and a short circuit current rise time of 12 µs. The standoff distance was provided by a 2.5 mm thick neoprene washer with an inside diameter of 19 mm and outside diameter of 37 mm. Due to the low strength of the neoprene washer, it broke and was ejected from between the flyer sheet and target plate. Six samples were created for this material combination. One of those samples was sectioned along the diameter and microhardness on either side of the weld interface was measured. Vicker's hardness of the base materials away from the interface was also measured.

3 Results and Discussion

3.1 Diagnostics

The time resolved current and voltage data from a 0.6 kJ shot on the fast bank and a 4 kJ shot on the slow bank are shown in **Fig. 3 (a)**. It can be noted that in the first case the

current reached the maximum value of 40 kiloamperes within 5 μs, while it took 13 μs for the current from the slow bank to reach the peak value of 100 kiloamperes. The voltage trace on the slow bank demonstrated a characteristic spike at the time of foil burst. This phenomenon could not be identified on the fast bank's discharge voltage trace.

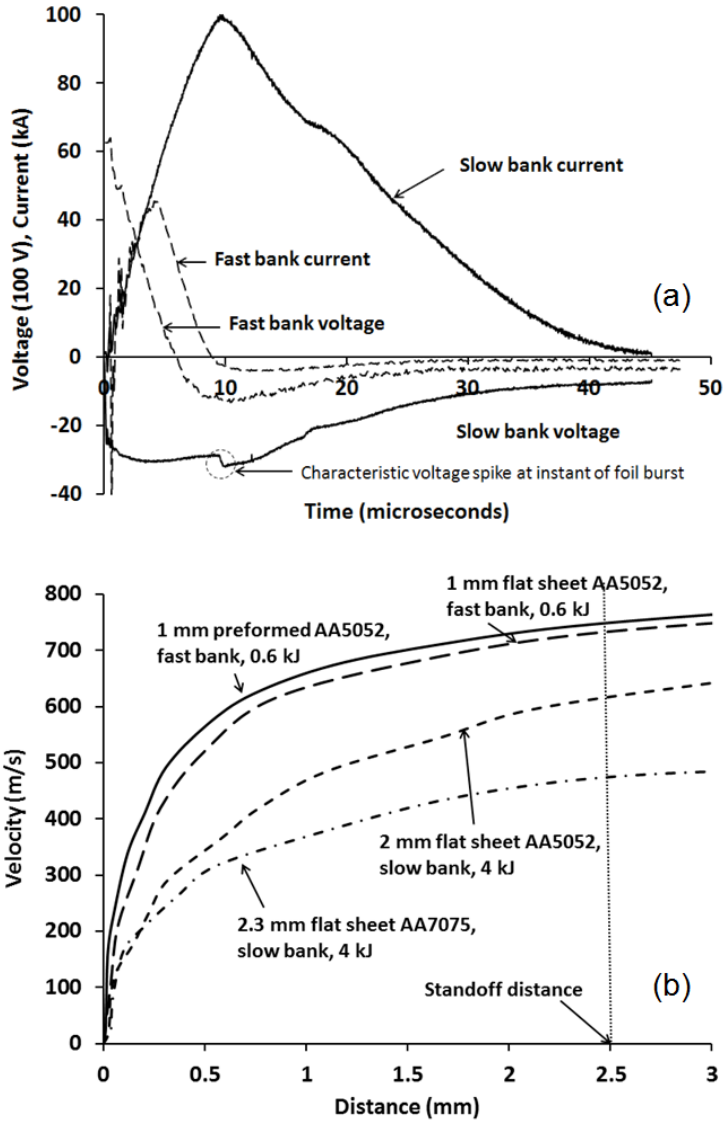

***Figure 3**: diagnostics on different types of experiments: (a) evolution of current and voltage with respect to time, (b) evolution of flyer sheet velocity with distance travelled.*

The evolution of flyer sheet velocities with distance travelled is illustrated in **Fig. 3 (b)**. As the impact with the target sheet occurred at a nominal distance of 2.5 mm, the impact velocities can be estimated as:

a) 1 mm flat sheet AA5052, fast bank at 0.6 kJ: 753 m/s
b) 1 mm preformed sheet AA5052, fast bank at 0.6 kJ: 731 m/s
c) 2 mm flat sheet AA5052, fast bank at 4 kJ: 569 m/s
d) 2.3 mm flat sheet AA7075, fast bank at 4 kJ: 472 m/s

3.2 AA5052 to AA5052

By creating spot welds at 0.6 kJ, truly low-energy impact welding of aluminium has been realized. RSW of aluminium consumes nearly one hundred times higher energy (Briskham et al., 2006). The use of a capacitor bank with a fast discharge frequency is important to achieve this energy efficiency. In a separate experiment not discussed here, it was observed that with the faster bank operating at 1 kJ energy level, a 1 mm thick AA5052 sheet can be launched to approximately 750 m/s within 2.5 mm of travel. The same launch carried out with a slower bank (12 μs current rise time) only achieved 400 m/s.

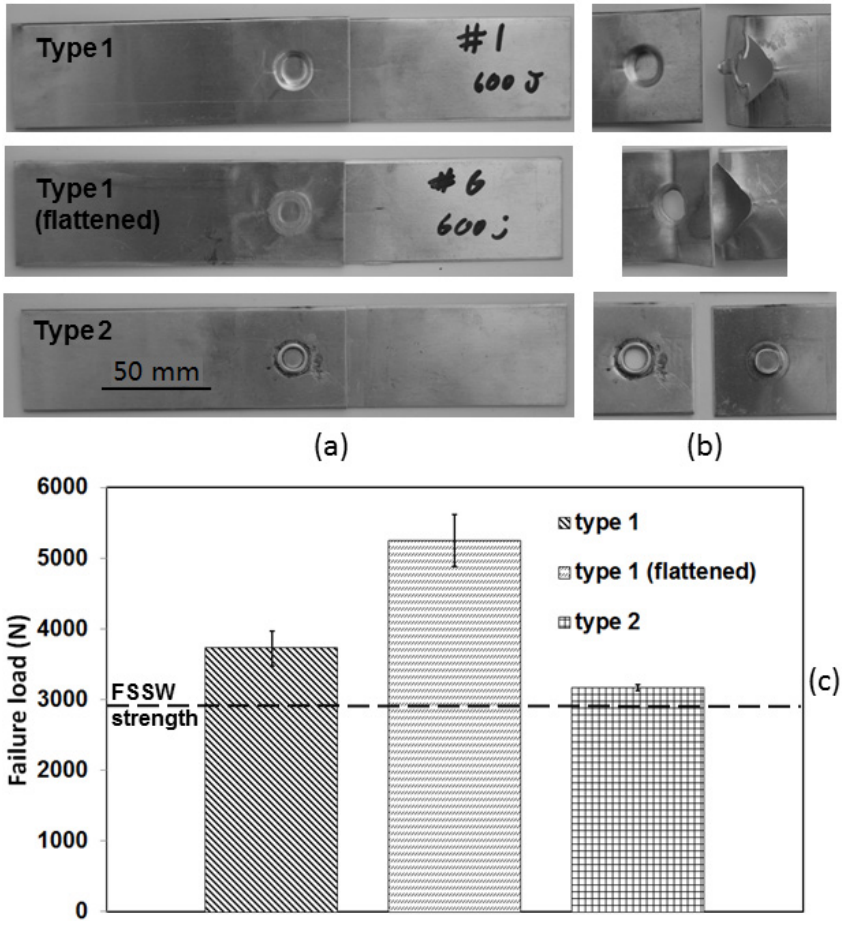

***Figure 4**: Similar alloy welds for AA5052: (a) before mechanical testing, (b) after mechanical testing , (c) failure loads from lap shear tests*

The average diameter of the spot welds was 10 mm. Most of the samples left behind a weld nugget upon mechanical testing. **Fig. 4** shows each type of sample before and after mechanical testing along with a graphical representation of the failure loads. The average failure load of as-welded type 1 samples was 3727 N with a standard deviation of 551 N. The average strength of the flattened type 1 samples was 5250 N with a standard deviation of 816 N. The type 2 samples failed at an average load of 3170 N with a standard deviation

of 39 N. It should be noted that all these failure loads are higher than the ones obtained with FSSW of similar material and spot size, which had lap shear strength of 2900 N (Zhang et al., 2011). The flattened type 1 sample showed the most improvement, where most of the samples sustained almost twice the load that the FSSW samples failed at. This can be attributed to the fact that the flattened type 1 samples had minimal thinning during the welding process and had no HAZ. One of the flattened type 1 samples failed along the interface at a lower load of 3505 N. This could have resulted from an experimental error in aligning the sheets, foil actuator and standoff insert before welding.

3.3 AA5052 to AA7075

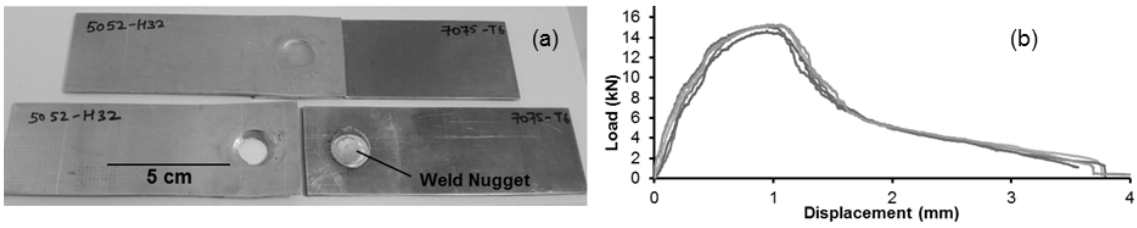

Figure 5*: (a) A5052/A7075 VFAW spot welded samples before and after lap shear testing, (b) a plot showing variation in load with stroke during lap shear testing of the welded samples.*

Fig. 5 (a) shows an impact spot-welded specimen before and after lap shear testing. The load vs. displacement data for each sample is plotted in **Fig. 5 (b)**. The samples failed outside the weld nugget reproducibly at an average load of 15.0 kN with a standard deviation of 286 N. The high strength of these welds can be attributed to three factors: (i) negligible thinning around the welded area, (ii) no HAZ and (iii) effective metallurgical joining with no gaps or cracks at the bond line. The weld cross-section image in **Fig. 6 (a)** depicts the characteristic wavy morphology of an impact welded interface in some parts of the weld. The figure also shows that the flyer sheet retained its original thickness in and around the weld. The microhardness data (**Fig. 6 (b)**) also reveals that the Vicker's hardness on both sides of the weld interface and around the weld nugget remained constant at the base material level, which is 90 HV for A5052 and 205 HV for A7075. This is due to the low external input energy to the weld. It turns out that the input energy for VFAW is not only an order of magnitude smaller than that for RSW, but is also merely a fraction of the energy required for friction spot welding or self-pierced riveting processes (Briskham et al., 2006).

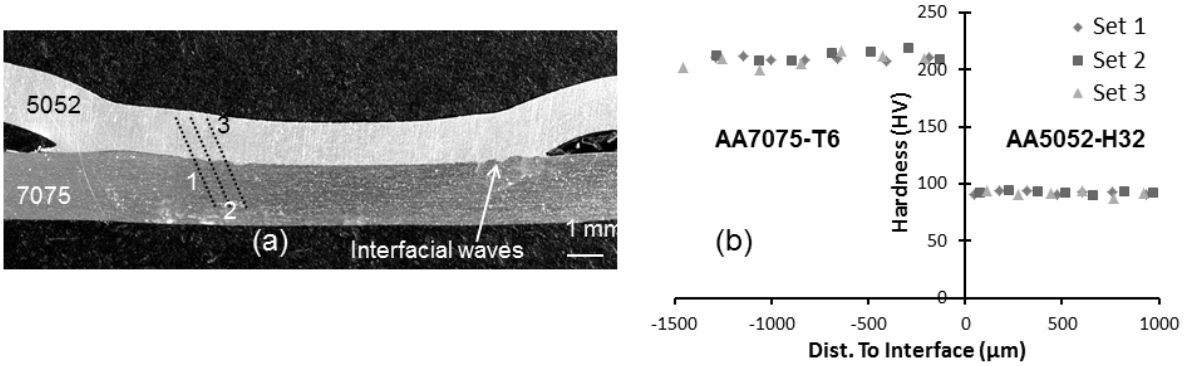

***Figure 6**: (a) Cross-section image of the welded sample depicting the lines along which microhardness testing was performed, (b) Test data showing constant microhardness on either sides of the weld interface.*

4 Conclusions

VFA spot welding of AA5052 to itself and to AA7075 was successfully implemented at very low input energies as compared to conventional welding processes. Upon mechanical testing, VFA spot weld samples failed outside the weld nugget and were significantly stronger than similar-sized FSSW. With minimal process-induced changes in geometric and mechanical properties of the base materials, VFAW enables approximately 100% joint efficiency, which sets it apart from other available joining techniques. This motivates further development of the process toward industrial implementation.

Acknowledgments

The authors are thankful for sponsorship from the ALCOA Foundation's Advancing Sustainability Research Initiative under grant no. GRT00025327. Materials were kindly provided by Honda R&D, North America.

References

Barnes, T. A., Pashby, I. R., 2000. Joining techniques for aluminum spaceframes used in automobiles. Part II - adhesive bonding and mechanical fasteners. Journal of Materials Processing Technology, 99, 72–79. doi:10.1016/S0924-0136(99)00361-1

Briskham, P., Blundell, N., Han, L., Hewitt, R., Young, K., Boomer, D., 2006. Comparison of self-pierce riveting , resistance spot welding and spot friction joining for aluminium automotive sheet. Sae Sp, 2034, 105. doi:10.4271/2006-01-0774

Grignon, F., Benson, D., Vecchio, K. S., Meyers, M. A., 2004. Explosive welding of aluminum to aluminum: analysis, computations and experiments. International Journal of Impact Engineering, 30(10), 1333–1351. doi:10.1016/j.ijimpeng.2003.09.049

Hahn, M., Weddeling, C., Taber, G., Vivek, A., Daehn, G. S., Tekkaya, a. E., 2016. Vaporizing foil actuator welding as a competing technology to magnetic pulse welding. Journal of Materials Processing Technology, 230, 8–20. doi:10.1016/j.jmatprotec.2015.11.010

Hwang, R. Y., Chou, C. P., 1998. The Study on Microstructural and Mechanical Properties of Weld Heat Affected Zone of 7075-T651 Aluminum Alloy. Scripta Materialia, 38(2), 215–221.

Lee, S. H., Saito, Y., Sakai, T., Utsunomiya, H., 2002. Microstructures and mechanical properties of 6061 aluminum alloy processed by accumulative roll-bonding. Materials Science and Engineering A, 325, 228–235. doi:10.1016/S0921-5093(01)01416-2

Loureiro, A. L., da Silva, L. F. M., Sato, C., Figueiredo, M. A. V., 2010. Comparison of the Mechanical Behaviour Between Stiff and Flexible Adhesive Joints for the Automotive Industry. The Journal of Adhesion, 86(July 2015), 765–787. doi:10.1080/00218464.2010.482440

Nandan, R., DebRoy, T., Bhadeshia, H. K. D. H., 2008. Recent advances in friction-stir welding - Process, weldment structure and properties. Progress in Materials Science, 53, 980–1023. doi:10.1016/j.pmatsci.2008.05.001

Vivek, A., Hansen, S. R., Liu, B. C., Daehn, G. S., 2013. Vaporizing foil actuator: A tool for collision welding. Journal of Materials Processing Technology, 213(12), 2304–2311. doi:10.1016/j.jmatprotec.2013.07.006

Watanabe, M., Kumai, S., 2009. Interfacial morphology of magnetic pulse welded aluminum/aluminum and copper/copper lap joints. Journal of Japan Institute of Light Metals, 59(2), 140–147. doi:10.2464/jilm.59.140

Zhang, C. (Sam), Deceuster, A., Li, L., 2009. A Method for Bond Strength Evaluation for Laminated Structures with Application to Ultrasonic Consolidation. Journal of Materials Engineering and Performance, 18(8), 1124–1132. doi:10.1007/s11665-008-9342-1

Zhang, Y., Babu, S. S., Prothe, C., Blakely, M., Kwasegroch, J., LaHa, M., Daehn, G. S., 2011. Application of high velocity impact welding at varied different length scales. Journal of Materials Processing Technology, 211(5), 944–952. doi:10.1016/j.jmatprotec.2010.01.001

Zhang, Z., Yang, X., Zhang, J., Zhou, G., Xu, X., Zou, B., 2011. Effect of welding parameters on microstructure and mechanical properties of friction stir spot welded 5052 aluminum alloy. Materials and Design, 32(8-9), 4461–4470. doi:10.1016/j.matdes.2011.03.058